Immunity, Vol. 15, 603–615, October, 2001, Copyright ©2001 by Cell Press

Gain- and Loss-of-Function Lyn Mutant Mice Define a Critical Inhibitory Role for Lyn in the Myeloid Lineage

Kenneth W. Harder,[1] Linda M. Parsons,[1] Jane Armes,[2,3] Natalie Evans,[1] Nicole Kountouri,[1] Roslyn Clark,[1] Cathy Quilici,[1] Dianne Grail,[1] George S. Hodgson,[1,5] Ashley R. Dunn,[1] and Margaret L. Hibbs[1,4]

[1]Ludwig Institute for Cancer Research
Melbourne Tumor Biology Branch
Royal Melbourne Hospital
Melbourne, Victoria 3050

[2]Melbourne Pathology
Royal Women's Hospital
Carlton, Victoria 3052

[3]Victorian Breast Cancer Research Consortium
University of Melbourne
Parkville, Victoria 3050
Australia

Summary

To investigate the role of the Lyn kinase in establishing signaling thresholds in hematopoietic cells, a gain-of-function mutation analogous to the Src Y527F-activating mutation was introduced into the *Lyn* gene. Intriguingly, although Lyn is widely expressed within the hematopoietic system, these mice displayed no propensity toward hematological malignancy. By contrast, analysis of aging cohorts of both loss- and gain-of-function *Lyn* mutant mice revealed that *Lyn*$^{-/-}$ mice develop splenomegaly, increased numbers of myeloid progenitors, and monocyte/macrophage (Mϕ) tumors. Biochemical analysis of cells from these mutants revealed that Lyn is essential in establishing ITIM-dependent inhibitory signaling and for activation of specific protein tyrosine phosphatases within myeloid cells. Loss of such inhibitory signaling may predispose mice lacking this putative protooncogene to tumorigenesis.

Introduction

A mutated version of c-Src, the prototypic member of the Src family of protooncogenes, is the dominantly acting oncogene encoded by the Rous sarcoma virus (Stehelin et al., 1976; Brugge and Erikson, 1977). Mutated versions of c-Src lacking a carboxy-terminal tyrosine phosphorylation site have the capacity to transform fibroblasts and illicit tumors in immunocompromised hosts. Similarly, gain-of-function mutants of other Src family kinases including Fyn, Yes, Fgr, Lck, and Hck possess the ability to transform cell lines either when introduced into such cells alone (reviewed by Brown and Cooper, 1996) or in combination with proteins such as HIV nef (Briggs et al., 1997; Moarefi et al., 1997).

Studies using standard transgenic technology have demonstrated that deregulated Src family kinase activity and expression can lead to tumorigenesis. For example, p56Lck^{Y505F} and p60Src^{Y527F} transgenic mice develop thymic lymphomas (Abraham et al., 1991) or mammary gland neoplasia, respectively (Webster et al., 1995). Similarly, transgenic mice expressing v-Src kinase under control of glial fibrillary acidic protein gene regulatory elements develop astrocytomas (Weissenberger et al., 1997), while H-2K promoter Blk^{Y495F} mutant transgenic mice develop lymphoid tumors (Malek et al., 1998). These studies, coupled with the observation that Src is essential for mammary tumor development in Neu transgenic mice, have contributed to the prevailing view that Src family kinases are participants in signaling pathways governing specific aspects of oncogenesis (Guy et al., 1994).

Although the Lyn tyrosine kinase has been reported to associate with many hematopoietic receptors including the BCR, FcεRI, CD14, and c-Kit among others (reviewed by Corey and Anderson, 1999), to date, analysis of *Lyn*$^{-/-}$ mice has focused on a phenotype largely limited to the B lymphoid compartment (Hibbs et al., 1995a; Nishizumi et al., 1995, 1998; Chan et al., 1997). Interestingly, these studies have revealed that although Lyn contributes to BCR-induced tyrosine phosphorylation, it has an indispensable role in phosphorylating specific tyrosine residues contained within immunoreceptor tyrosine-based inhibitory motifs (ITIM) in the cytoplasmic domains of inhibitory receptors such as CD22 (Smith et al., 1998; Cornall et al., 1998), PIR-B (Maeda et al., 1998; Ho et al., 1999), and FcγRIIB (Chan et al., 1997, 1998; Nishizumi et al., 1998). Consequently, B cells lacking Lyn fail to recruit the PTP SHP-1 and the SH2-containing 5′-inositol phosphatase (SHIP-1) to the plasma membrane in response to appropriate stimuli. These signaling deficiencies are thought to underpin the *Lyn*$^{-/-}$ mouse B lymphoid phenotype which includes reduced levels of mature B cells, hyper-IgM, hyperresponsive BCR-dependent proliferation, diminished FcγRIIB1-dependent signal inhibition, and production of autoreactive antibodies culminating in immune complex deposition in the kidneys (Hibbs et al., 1995a; Nishizumi et al., 1995, 1998; Chan et al., 1997).

In studies aimed at investigating the role of Lyn in murine hematopoietic system development and directly assessing its positive versus negative signaling roles, a gain-of-function mutation was introduced into the *Lyn* locus. The gain-of-function knockin mutant, like the naturally occurring RSV Src mutant, lacks a critical tyrosine phosphorylation site at the C terminus required for negative regulation of kinase activity, and is thus constitutively active.

Our studies of aged Lyn mutant mice (both loss- and gain-of-function) reveal that Lyn-deficient mice develop a dramatic increase in myeloid progenitors, splenomegaly, and disseminated monocyte/Mϕ tumors while Lyn gain-of-function mice are tumor free. Overall, this study demonstrates that loss of the Lyn kinase leads to tumor development and highlights a critical role for this tyrosine kinase in establishing phosphatase-dependent inhibitory signaling pathways in the monocyte/Mϕ compartment of the hematopoietic system. This data establishes a new paradigm for the role of a Src family member in tumorigenesis.

[4]Correspondence: margaret.hibbs@ludwig.edu.au

[5]Deceased.

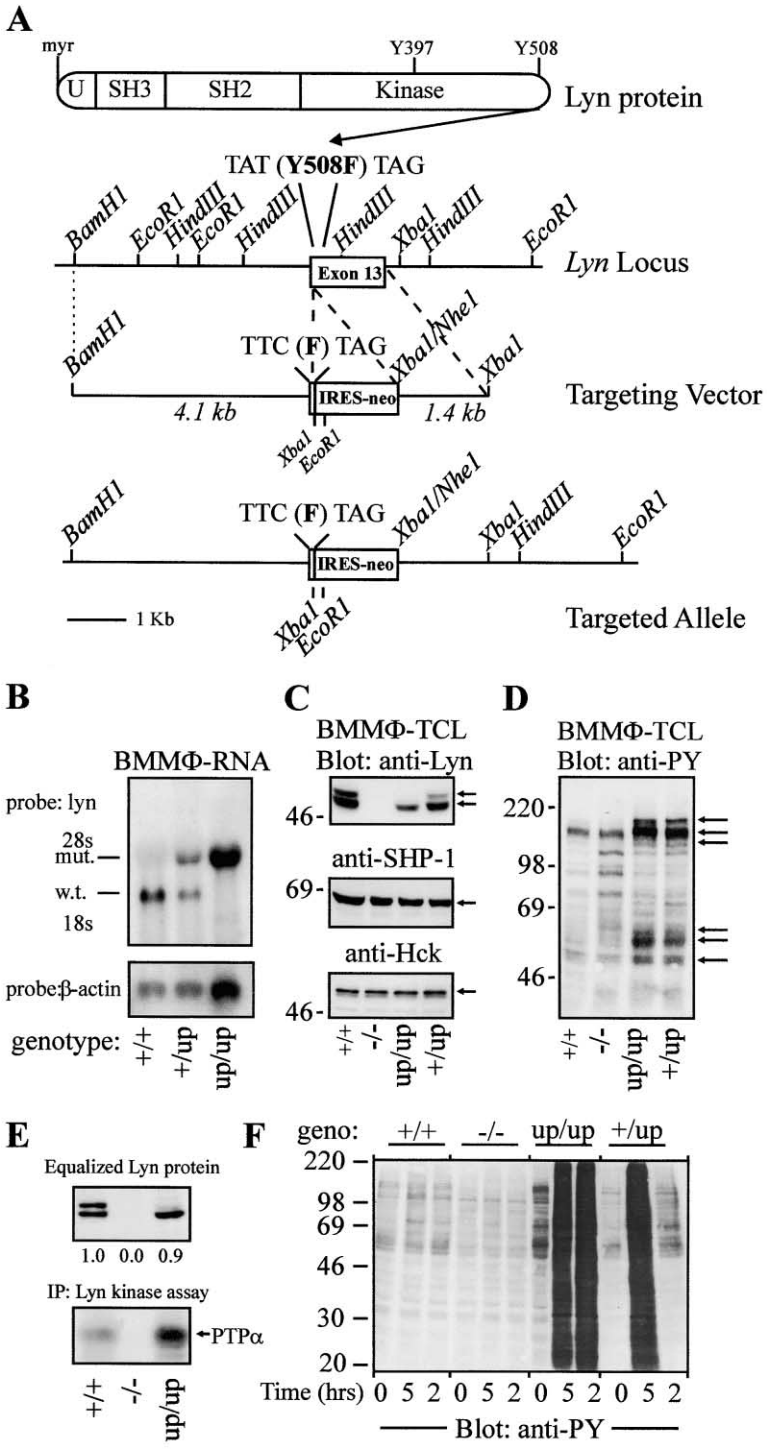

Figure 1. Generation of the Lyn Gain-of-Function (*Lyn*^{up}) Mutant Mouse

(A) Lyn kinase protein structure and targeting vector for modification of the *Lyn* gene. The 3′ end of the mouse *Lyn* locus, the targeting vector, and recombinant *lyn* knockin allele are shown. Exon 13 containing Y508 is depicted as a box.

(B) Total RNA from *Lyn*$^{+/+}$, *Lyn*$^{+/up}$, and *Lyn*$^{up/up}$ BMMϕs was probed with the *Lyn* cDNA (upper panel). The predicted size of the wild-type (w.t.) *Lyn* (3.4 kb) and the IRES-neo cassette containing *Lyn* mutant (mut.) (4.8 kb) mRNAs are indicated. A β-actin probe was used to assess loading (lower panel).

(C) Total cell lysates (TCL) from BMMϕs derived from mice of the indicated genotypes were blotted with anti-Lyn Abs. The blot was then stripped and reblotted with anti-SHP-1 or anti-Hck Abs to ensure equal protein loading. Arrows indicate the positions of the p56 and p53 Lyn isoforms, or those of SHP-1 and Hck.

(D) BMMϕ TCLs shown in Figure 1C were stripped and blotted with anti-PY Abs. Arrows indicate proteins exhibiting enhanced anti-PY immunoreactivity in *Lyn*$^{up/up}$ and *Lyn*$^{+/up}$ samples.

(E) Assessment of Lyn kinase activity. Lyn kinase was precipitated from lysates containing equalized amounts of Lyn (upper panel, with densitometry values) and subjected to an immune complex kinase assay in the presence of recombinant PTPα domain 2 substrate.

(F) BMMϕs from the indicated mice were treated with pervanadate for the times shown and TCLs were blotted with anti-PY Abs.

Results

Generation of *Lyn*^{Y508F} (*Lyn*^{up}) Gain-of-Function Mutant Mice

A gain-of-function mutation in *Lyn* was introduced into the mouse germline by homologous recombination in ES cells. Site-directed mutagenesis was used to introduce the Tyr-to-Phe activating mutation at residue 508 (*Lyn*^{Y508F}, hereafter referred to as *Lyn*^{up}) into the murine *Lyn* gene (exon 13) along with an IRES neomycin cassette (Figure 1A). A Northern blot of total RNA isolated from bone marrow macrophages (BMMϕs) confirmed expression of the bicistronic message in both *Lyn*$^{up/up}$ and *Lyn*$^{+/up}$ cells (Figure 1B). Immunoblots of total cell lysates (TCL) from BMMϕs with Lyn-specific antibodies (Abs) established Lyn^{up} protein expression. However, reduced levels of Lyn^{up} protein, and in particular the p56 isoform, were detected in *Lyn*$^{up/up}$-derived BMMϕs and

other primary cell types (Figure 1C and data not shown). Reduced levels of Lyn^{up} protein were observed regardless of the detergent used to produce cell lysates. Immunoblotting with SHP-1- and Hck-specific antisera revealed similar levels of both of these proteins in the BMMϕs (Figure 1C, panels 2 and 3). Our preliminary data suggest that the activated form of Lyn, like other activated Src kinase mutants, is subject to ubiquitin-dependent degradation (data not shown; Oda et al., 1999; Hakak and Martin, 1999; Harris et al., 1999). Despite reduced levels of Lyn^{up} protein, increased levels of overall tyrosine phosphorylation were observed following antiphosphotyrosine (PY) immunoblotting of BMMϕ TCLs (Figure 1D). Moreover, kinase assays performed on equalized levels of Lyn protein revealed a 2- to 3-fold increase in the specific activity of the Lyn^{up} protein (Figure 1E).

It is well established that the activity of tyrosine kinases and their substrates is tightly regulated by the opposing activity of a large family of PTPs. To assess the contribution of PTP activity to the relatively modest increase in overall tyrosine phosphorylation in Lyn^{up}-derived cells, we investigated the sensitivity of *Lyn^{up}* mutant cells to the PTP inhibitor pervanadate. BMMϕs were treated with modified pervanadate (100 μM Vn; 2 μM H_2O_2) and levels of tyrosine phosphorylation in TCLs were analyzed (Figure 1F). Both the *Lyn$^{up/up}$* and *Lyn$^{+/up}$* cells exhibited dramatically enhanced levels of tyrosine phosphorylation following pervanadate treatment. By contrast, both *Lyn$^{+/+}$* and *Lyn$^{-/-}$* BMMϕs were apparently unaffected by this dose of drug. These results, combined with the elevated levels of anti-PY immunoreactivity detected in lysates from *Lyn$^{up/up}$* and *Lyn$^{+/up}$* BMMϕs, confirm that the Y508F substitution introduced into the *Lyn* gene results in a gain-of-function Lyn kinase mutant.

Age-Dependent Development of Splenomegaly and Disseminated Myelomonocytic Cells in *Lyn$^{-/-}$* but Not *Lyn$^{up/up}$* Mice

To investigate Lyn's role in signal transduction/inhibition and to directly assess the oncogenic potential of the Lyn gain-of-function mutant, a cohort of *Lyn$^{+/+}$*, *Lyn$^{-/-}$*, and *Lyn$^{up/up}$* mice was investigated for age-dependent differences in various hematopoietic parameters (see supplemental table at http://www.immunity.com/cgi/content/full/15/4/603/DC1) and the cellular composition of spleen and bone marrow (BM). As previously observed, *Lyn$^{-/-}$* mice developed an age-dependent increase in spleen weight (Supplemental Table S1; Nishizumi et al., 1995; Chan et al., 1997), a phenotype that is at least partially dependent on the Btk kinase (Takeshita et al., 1998; Satterthwaite et al., 1998). By contrast, *Lyn$^{up/up}$* mouse spleen weights were modestly lower than those of *Lyn$^{+/+}$* mice (due to specific *Lyn$^{up/up}$* B-lymphoid differences; our unpublished data). We also observed a decrease in platelet numbers in *Lyn$^{-/-}$* mice which became more pronounced with age (Supplemental Table S1). Flow cytometry analyses of *Lyn$^{up/up}$* blood, spleen, and BM were unremarkable in terms of the myeloid compartment with the exception of an increase in the numbers of neutrophils in spleen and peripheral blood of *Lyn$^{up/up}$* mice. For example, peripheral blood neutrophil

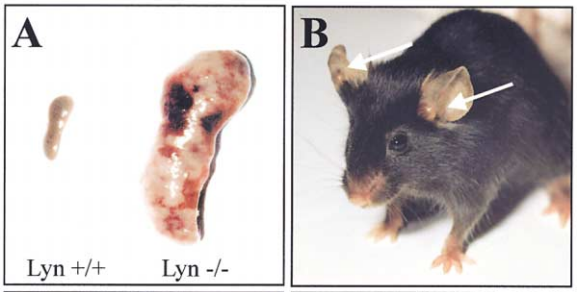

E

Lyn$^{-/-}$ (donor) → 1°SCID → 2°SCID

#	spleen (g)	1°SCID incidence	1°SCID latency	2°SCID incidence	2°SCID latency
1	4.2	4/4	10-12wks	4/4	10-12
2	1.5	1/2*	5	2/3	13
3	4.1	3/3	20-29		
4	3.2	2/2	9		
5	1.9	2/2	18		

Figure 2. *Lyn$^{-/-}$* Mice Develop Severe Splenomegaly and Disseminated Mϕ Tumors that Can Be Transferred into SCID Mouse Recipients

(A) Spleens from age-matched 18-month-old *Lyn$^{+/+}$* (0.08 g) and *Lyn$^{-/-}$* (3.21 g) mice.

(B) An example of tumors on the ears of a *Lyn$^{-/-}$* mouse.

(C) A mass of cells on the tail of a *Lyn$^{-/-}$* mouse.

(D) Transmission EM of cells comprising the tail mass in (C), original magnification 5.0 K. The scale bar represents 10 μm.

(E) Single-cell suspensions from spleens from *Lyn$^{-/-}$* mice exhibiting various degrees of splenomegaly were injected into 13 female SCID mouse recipients and tumor latency was assessed. Spleen cell suspensions from two tumor-bearing primary SCID mice (seeded with cells from *Lyn$^{-/-}$* donor #1) were injected into a total of seven secondary SCID mouse recipients and tumor latency was determined. The asterisk represents those found dead.

counts for 6- to 8-week-old mice were: *Lyn$^{+/+}$*, 609 $\pm$ 207/μl; *Lyn$^{up/up}$*, 1089 $\pm$ 242/μl (n = 12); and for 52- to 58-week-old mice: *Lyn$^{+/+}$*, 1262 $\pm$ 434/μl; *Lyn$^{up/up}$*, 2540 $\pm$ 1050/μl (n = 8).

Splenomegaly became severe (>0.5 g) in approximately 20% of *Lyn$^{-/-}$* mice greater than 1 year of age with partial or almost complete replacement of the red and white pulp by atypical myelomonocytic cells often admixed with centers of extramedullary hematopoiesis (EMH; Figures 2A and 3A). Enlargement of the spleens of *Lyn$^{-/-}$* mice was also frequently associated with disseminated accumulations of myelomonocytic cells in the liver and lymph nodes. These cells were also com-

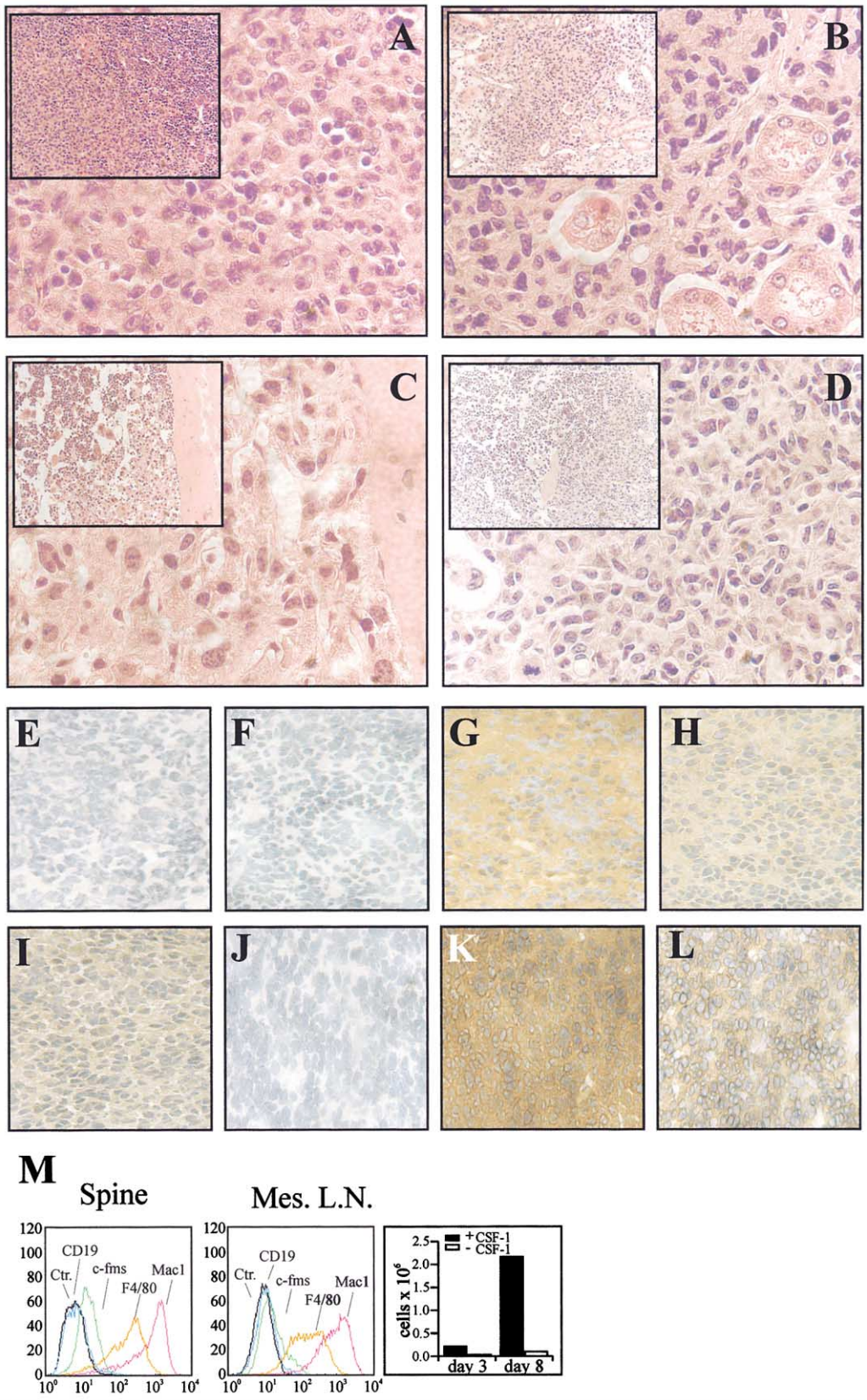

Figure 3. Histological and Immunohistochemical Analysis of *Lyn*$^{-/-}$ Mice, Tumor-Bearing SCID, and *Lyn*$^{-/-}$/μ*MT*/μ*MT* Mice

(A–D) Histological analysis of tumor-bearing *Lyn*$^{-/-}$ mice. A Mϕ/histiocytic tumor in the spleen of a *Lyn*$^{-/-}$ mouse (A). Mϕ/histiocytic tumors in the kidney (B) and BM (C) of SCID mouse recipients of *Lyn*$^{-/-}$ spleen-derived donor cells. Expansion of Mϕ/histiocytic tumor in the BM of a *Lyn*$^{-/-}$/μ*MT*/μ*MT* mouse (D).

monly observed in aged *Lyn*$^{-/-}$ mice with mild splenomegaly. Accumulation of such cells was often observed in lungs, BM, connective tissue, ovaries, pancreas, bowel, and kidneys, with some cells exhibiting atypical mitoses, highly suggestive of malignancy (data not shown). Intriguingly, older *Lyn*$^{-/-}$ mice sporadically developed large aggregates of myelomonocytic cells on the tail, ears, and legs (Figures 2B and 2C). These cells were phenotypically similar to those disseminated throughout other organs. Transmission electron microscopy (EM) of these masses revealed cells with a mean diameter of 45.3 $\pm$ 4.8 μm that were rich in mitochondria and lysosomes (Figure 2D). Some cells in the fields also exhibited pseudopodia. Notably absent were any cells indicative of infection.

Transplantability of Monocyte/Mϕ Tumors into SCID Mice and Tumor Development in *Lyn*$^{-/-}$/μ*MT*/μ*MT* Mice

We assessed the tumorigenic potential of the myelomonocytic population in *Lyn*$^{-/-}$ mice by injecting splenic cells from *Lyn*$^{-/-}$ mice into SCID mice (Figure 2E). Donor cells derived from five *Lyn*$^{-/-}$ mice exhibiting splenomegaly were injected into 13 female SCID mice. All recipients (except one that was found dead) developed Mϕ tumors with latencies ranging from 5 to 29 weeks and developed splenomegaly (0.14–1.7 g). Furthermore, when single-cell suspensions of tumor-containing spleens from two primary SCID recipients seeded with cells from *Lyn*$^{-/-}$ donor number 1 were injected into a total of seven secondary SCID mice, six of these mice developed tumors with a similar latency to the primary recipients. Spleen weights of these recipients ranged from 0.21 to 0.83 g.

Detailed histological examination of injected SCID mice revealed tumor in the spleens of all but two recipients (12/14). Tumor deposits were also observed in liver (13/14), lungs (8/14), perinephric fat (8/14), BM (11/14), and lymph nodes. A section of a recipient SCID mouse illustrates monocytoid/histiocytic expansions in kidney and BM (Figures 3B and 3C). Tumor in the BM varied from almost complete replacement to small focal deposits. Confirmation that these cells were derived from donor *Lyn*$^{-/-}$ mice was obtained by PCR to detect the *Lyn* knockout allele (data not shown).

Lyn$^{-/-}$ mice have high serum IgM and self-reactive Abs that with age result in a severe kidney pathology (Hibbs et al., 1995a; Nishizumi et al., 1995). Others have suggested that *Lyn*$^{-/-}$ mice also develop an expansion of Mac1^{+}/CD5^{+} B1-B cells in lymphoid organs (Chan et al., 1997) and an atypical splenic B cell population containing cytoplasmic Ig (Nishizumi et al., 1995). To investigate whether tumor development was dependent on B cell-dependent autoimmunity in *Lyn*$^{-/-}$ mice and to preclude the possibility of a B cell tumor classification, we produced *Lyn*$^{-/-}$/μ*MT*/μ*MT* mice. Despite the lack of mature B cells due to disruption of the μ chain transmembrane domain-encoding exon, these double mutant mice developed tumors indistinguishable from *Lyn*$^{-/-}$ mice as evidenced by an expansion of Mϕ/histiocytes in the *Lyn*$^{-/-}$/μ*MT*/μ*MT* femur shown (Figure 3D).

Characterization of *Lyn*$^{-/-}$ Mouse Mϕ Tumors

Lyn$^{-/-}$ tumor cells were characterized by immunohistochemistry with monoclonal antibodies (mAbs) specific for granulocyte, Mϕ, or lymphocyte cell surface markers. Tumor cells stained strongly with mAbs against the myeloid marker Mac-1 (Figure 3G) and the more restricted Mϕ marker F4/80 (Figure 3H), and to a lesser degree with Abs toward the granulocytic/monocytic marker Ly6G (Gr-1; Figure 3I). The sections did not stain with isotype control Abs (Figure 3E) or with B or T cell-specific markers such as B220 (Figure 3F), CD19, or Thy-1 (data not shown). Immunohistochemistry of tumor-bearing SCID mice confirmed the myeloid nature of the transplanted tumor (data not shown). Both B and T cell-specific staining of tumor tissue and FACS analysis of cells obtained from such tissues failed to detect significant numbers of either cell type. Similarly, immunohistochemical analysis of sections of microdissected tumors associated with the spine and mesenteric lymph nodes of a *Lyn*$^{-/-}$/μ*MT*/μ*MT* mouse, like those of *Lyn*$^{-/-}$ mice, stained with mAbs specific for Mac-1 and F4/80 (Figures 3K and 3L), but not with isotype control (Figure 3J) or B220 and Thy-1 mAbs (data not shown).

Ex vivo analysis of these cells provided further evidence of the monocyte/Mϕ origin of the tumor cells. Tumor cells prepared from the spine and mesenteric lymph node of a *Lyn*$^{-/-}$/μ*MT*/μ*MT* mouse and grown ex vivo stained with Mϕ markers (Mac-1^{+}, c-fms^{low}, and F4/80^{+}), lacked B cell marker expression (CD19^{-}), and were dependent on CSF-1 for their growth in vitro (Figure 3M). Taken together, the transmission EM, general histology, immunohistochemistry, FACS analysis, and CSF-1 dependence in vitro are supportive of a Mϕ (or histiocytic) classification for these cells.

Increased Myeloid Progenitors in Spleen and Peripheral Blood of *Lyn*$^{-/-}$ Mice

The development of disseminated Mϕ tumors in older *Lyn*$^{-/-}$ mice and their growth in SCID mice prompted us to investigate whether deregulated myelopoiesis might be a preexisting subpathological condition in younger *Lyn*$^{-/-}$ mice. We assessed numbers of myeloid progenitors in the spleen, BM, and peripheral blood of *Lyn*$^{+/+}$, *Lyn*$^{-/-}$, and *Lyn*$^{up/up}$ mice. Both splenic and peripheral blood M-CFCs were dramatically enhanced in the blood (8 weeks) and spleen (16 weeks) of *Lyn*$^{-/-}$ mice (Figures 4A and 4B). The spleens of *Lyn*$^{-/-}$ mice also exhibited enhanced CFU-GM, CFU-G, CFU-IL3, and CFU-SCF col-

(E–L) Immunohistochemical analysis of *Lyn*$^{-/-}$ tumors. Cryostat sections from a tumor on the ear of a *Lyn*$^{-/-}$ mouse were stained with isotype control (E); B220 (F); Mac-1 (G); F4/80 (H); and Gr-1 (I). An enlarged mesenteric lymph node mass from a *Lyn*$^{-/-}$/μ*MT*/μ*MT* mouse was stained with isotype control (J); Mac-1 (K); and F4/80 (L).

(M) Microdissected tumors associated with the spine and mesenteric lymph node from the same *Lyn*$^{-/-}$/μ*MT*/μ*MT* mouse analyzed in (J–L) were passed through a mesh, and single-cell suspensions were analyzed by FACS for cell surface marker expression (left and middle panels). Cells were grown for 3 or 8 days in either the presence or absence of CSF-1 and counted (right panel).

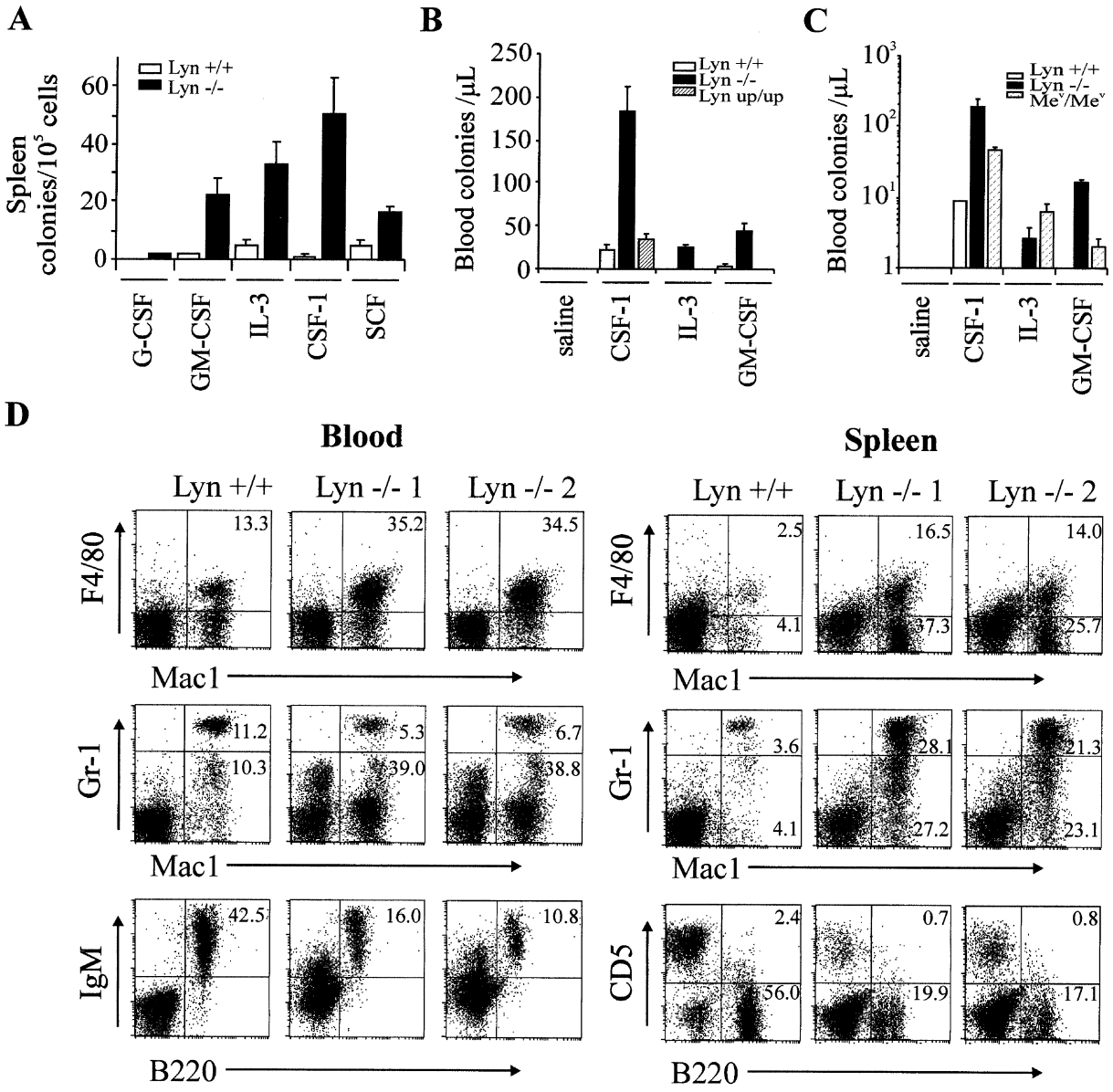

Figure 4. *Lyn*$^{-/-}$ Mice Possess Increased Numbers of Myeloid Progenitors, Splenic Myeloid Cells, and Peripheral Blood Monocytes

(A) Splenic progenitors in *Lyn*$^{-/-}$ (closed bars) and *Lyn*$^{+/+}$ mice (open bars) were assessed by in vitro semisolid agar assays in the presence of the indicated cytokines. Numbers shown are the mean ± standard error of the mean (SEM) for two groups of three 16-week-old mice in two separate experiments.

(B) Peripheral blood progenitor populations were determined in *Lyn*$^{+/+}$ (open bars), *Lyn*$^{-/-}$ (closed bars), and *Lyn*$^{up/up}$ (hatched bars) mice as above. Values represent the mean ± SEM of triplicate determinations for at least two mice per group.

(C) Peripheral blood progenitors in *Lyn*$^{+/+}$, *Lyn*$^{-/-}$, and *Me*^{v}/*Me*^{v} mice were assessed as in (B).

(D) FACS analysis of peripheral blood and splenic single-cell suspensions from 35-week-old *Lyn*$^{+/+}$ and *Lyn*$^{-/-}$ mice. Spleen weights were *Lyn*$^{+/+}$, 0.086 g; *Lyn*$^{-/-}$1, 0.534 g; and *Lyn*$^{-/-}$2, 0.486 g. WBC counts were similar: *Lyn*$^{+/+}$, 8.4 × 10^6/ml; *Lyn*$^{-/-}$1, 8.4 × 10^6/ml; and *Lyn*$^{-/-}$2, 8.0 × 10^6/ml.

onies as compared to age-matched *Lyn*$^{+/+}$ mice (Figure 4A). By contrast, the frequencies of BM CFU-M and CFU-GM progenitor populations were similar among the genotypes (data not shown). Peripheral blood progenitor numbers in *Lyn*$^{up/up}$ mice were similar to those of *Lyn*$^{+/+}$ mice (Figure 4B).

Some features of the phenotype of *Lyn*$^{-/-}$ mice are similar to those exhibited by mice deficient in specific signal-inhibitory proteins. For example, *Me*^{v}/*Me*^{v} and *SHIP-1*$^{-/-}$ mutant mice both develop splenomegaly and EMH, and have elevated progenitor numbers (Van Zant and Shultz, 1989; Helgason et al., 1998; Liu et al., 1999). Comparisons between age-matched 7- to 9-week-old *Me*^{v}/*Me*^{v} and *Lyn*$^{-/-}$ mice showed a dramatic enhancement in CFU-M in the peripheral blood of both mouse mutants (Figure 4C). Strikingly, *Lyn*$^{-/-}$ mice exhibited

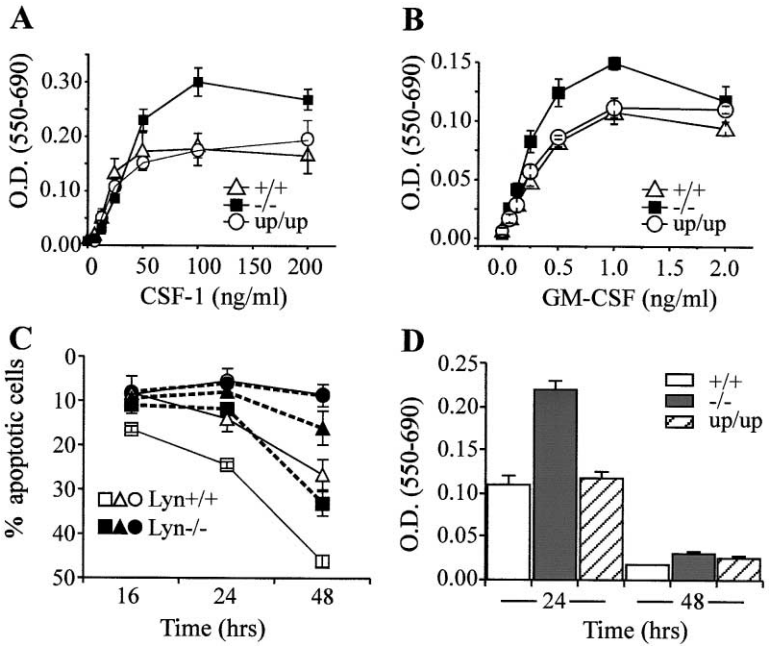

Figure 5. *Lyn*$^{-/-}$ BMMϕs Are Hypersensitive to CSF-1 and GM-CSF

(A and B) *Lyn*$^{+/+}$, *Lyn*$^{-/-}$, and *Lyn*$^{up/up}$ BMMϕ cell numbers were assessed in either CSF-1 (A) or GM-CSF (B). Relative cell numbers were determined by MTT assay. Each point represents the mean ± standard deviation (SD) of triplicate wells.

(C) The relative survival of BMMϕs from *Lyn*$^{+/+}$ (open symbols) and *Lyn*$^{-/-}$ (closed symbols) mice was assessed at 16, 24, and 48 hr in either the absence of added factor (open square/closed square), 2 ng/ml GM-CSF (open circle/closed circle), or 0.02 ng/ml GM-CSF (open triangle/closed triangle). Points represent the mean ± SD of duplicate wells.

(D) BMMϕ survival in the absence of growth factor at 24 and 48 hr. Relative cell numbers were assessed by MTT assay (*Lyn*$^{+/+}$, open bars; *Lyn*$^{-/-}$, closed bars; *Lyn*$^{up/up}$, hatched bars). Assays were performed in quadruplicate and values represent the mean ± SD.

greater numbers of peripheral blood Mϕ progenitors than did *Me*^{v}/*Me*^{v} mice (Figure 4C). Enhanced myeloid progenitors were also observed in the presence of IL-3 and GM-CSF in both *Lyn*$^{-/-}$ and *Me*^{v}/*Me*^{v} mice.

In keeping with the observed increase in splenic and peripheral blood CFU-M and CFU-GM progenitor numbers, FACS analysis of spleen and peripheral blood of 35-week-old *Lyn*$^{-/-}$ mice detected increased proportions of neutrophils (Mac-1^{+}/Gr-1^{+}) and Mϕs (Mac-1^{+}/F4/80^{+}) in the spleens, and increased numbers of monocytes in the peripheral blood of *Lyn*$^{-/-}$ mice (Figure 4D). We were unable to detect any evidence for increased numbers of either conventional or B1-B cells in the spleen (Figure 4D, B220/CD5 profiles) or peripheral blood (Figure 4D, B220/IgM profiles) of *Lyn*$^{-/-}$ mice. Indeed, as we have reported previously, levels of mature B cells were reduced in *Lyn*$^{-/-}$ mice (Hibbs et al., 1995a).

Enhanced Sensitivity of *Lyn*$^{-/-}$ BMMϕs to CSF-1 and GM-CSF

The dramatic increase in Mϕ progenitors and accumulation of Mϕ tumors in *Lyn*$^{-/-}$ mice led us to hypothesize that *Lyn*$^{-/-}$ Mϕ and/or their precursors might be hyperresponsive to cytokines and/or resistant to apoptosis. Previous reports have shown that Mϕs derived from motheaten mice are hyperresponsive to GM-CSF and CSF-1 due to lack of inhibition normally exerted by the PTP SHP-1 on cytokine-dependent signal transduction (Chen et al., 1996; Jiao et al., 1997). To investigate whether Lyn might also have an essential inhibitory signaling role in Mϕ, we compared the CSF-1 and GM-CSF sensitivity of BMMϕs from *Lyn*$^{+/+}$, *Lyn*$^{-/-}$, and *Lyn*$^{up/up}$ mice. Although *Lyn*$^{+/+}$ and *Lyn*$^{up/up}$ cells showed similar cytokine dose responses, *Lyn*$^{-/-}$ cells appeared to be moderately more sensitive to both CSF-1 and GM-CSF (Figures 5A and 5B). Others have demonstrated that *Me*/*Me* BMMϕs are profoundly resistant to cytokine withdrawal-induced apoptosis (Berg et al., 1999). However, *Lyn*$^{-/-}$ BMMϕs were only modestly less susceptible to apoptosis induced by cytokine withdrawal or suboptimal doses of GM-CSF (Figures 5C and 5D) and CSF-1 (data not shown). No difference between *Lyn*$^{+/+}$ and *Lyn*$^{up/up}$ cells was observed in these assays (Figure 5D and data not shown). Together, these results show that Mϕs from *Lyn*$^{-/-}$ mice are hyperresponsive to cytokines and subtly resistant to cytokine withdrawal-induced apoptosis.

Lyn-Dependent Regulation of SHP-1/SHIP-1, and SHP-1 and SHP-2 Association with Specific ITIM-Bearing Receptors within Mϕs

The development of Mϕ tumors and elevated Mϕ progenitors in *Lyn*$^{-/-}$ mice, coupled with the phenotypic similarities of *Lyn*$^{-/-}$, *Me*^{v}/*Me*^{v}, and *SHIP-1*$^{-/-}$ mice, led us to suspect that Lyn might be critical for phosphatase-dependent inhibitory signaling in myeloid cells. In addition, elevated tyrosine phosphorylation levels in specific proteins were consistently observed in TCLs derived from *Lyn*$^{-/-}$ BMMϕs suggestive of reduced phosphatase activity in these cells (Figure 1D). To investigate the role of Lyn in phosphatase regulation, SHP-1 and SHIP-1 were precipitated from BMMϕ and peripheral blood-derived Mϕ lysates (PBDMϕs) and assessed for differential tyrosine phosphorylation and/or associations with other proteins. Both SHP-1 and SHIP-1 exhibited elevated levels of tyrosine phosphorylation in *Lyn*$^{up/up}$-derived BMMϕs, and were correspondingly hypotyrosine phosphorylated in *Lyn*$^{-/-}$ cells (Figure 6A, upper left and upper right panels). Thus, these results demonstrate that the Lyn kinase regulates the tyrosine phosphorylation status of SHP-1 and SHIP-1 in primary cells, an observation consistent with in vitro and exogenous expression studies (Yoshida et al., 1999; Phee et al., 2000). In *Lyn*$^{up/up}$-derived BMMϕs, SHP-1 coprecipitated a tyro-

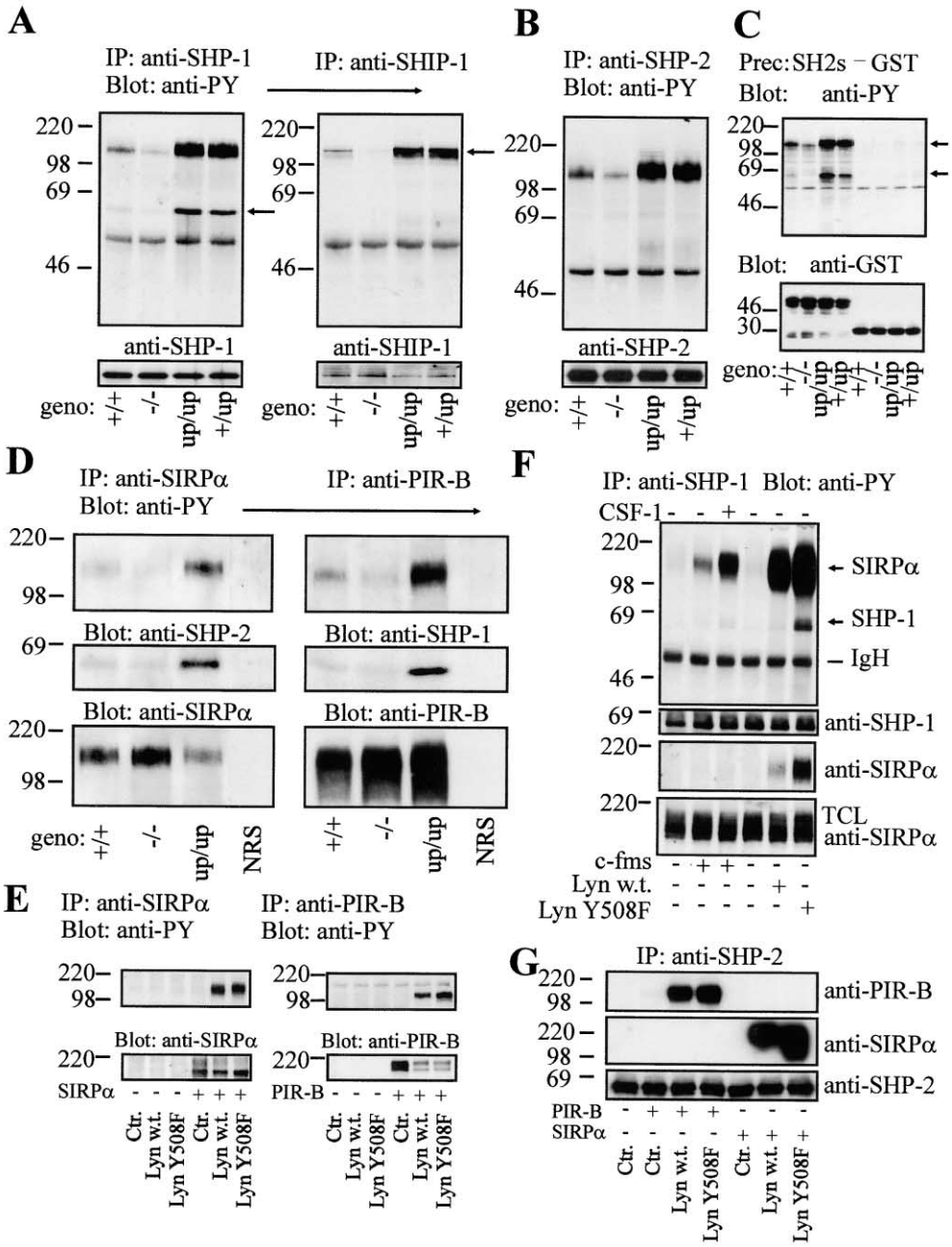

Figure 6. Lyn-Dependent Regulation of SHP-1/SHIP-1 Tyrosine Phosphorylation and Phosphatase Association with ITIM-Bearing Inhibitory Receptors

(A) SHP-1 (upper left panel) and SHIP-1 (upper right panel) were precipitated from $Lyn^{+/+}$, $Lyn^{-/-}$, $Lyn^{up/up}$, and $Lyn^{+/up}$ BMMϕ lysates and blotted with anti-PY, anti-SHP-1, or anti-SHIP-1 Abs. Arrows indicate the positions of SHP-1 and SHIP-1.

(B) SHP-2 was precipitated from BMMϕ lysates and blotted with anti-PY (upper panel) or anti-SHP-2 Abs (lower panel).

(C) Lysates of BMMϕs from control or Lyn mutant mice were incubated with purified fusion proteins containing the tandem SH2 domains of SHP-2 fused to GST or GST alone. Precipitates were then blotted with either anti-PY (upper panel) or anti-GST Abs (lower panel).

(D) SIRPα (left panels) and PIR-B (right panels) were precipitated from $Lyn^{+/+}$, $Lyn^{-/-}$, and $Lyn^{up/up}$ BMMϕ lysates and blotted with the Abs indicated. Lysates were also subject to normal rabbit serum (NRS) precipitations and blotted with the indicated Abs.

(E) 293T cells were cotransfected with SIRPα (left panels) or PIR-B (right panels) together with either control vector (Ctr.) or expression vectors containing the wild-type or Y508F mutant form of Lyn. SIRPα and PIR-B were then precipitated and blotted with anti-PY, SIRPα, or PIR-B Abs.

(F) 293T cells were transfected with SHP-1 and SIRPα together with the indicated expression vectors. Cells stimulated with CSF-1 (100 ng/ml) are indicated by a (+) symbol. SHP-1 was precipitated from lysates of the transfected cells and blotted with the indicated Abs. SIRPα protein levels in TCLs are shown in an anti-SIRPα blot (bottom panel).

(G) 293T cells were transfected with the plasmids outlined and SHP-2 was precipitated from lysates of these cells and blotted with anti-PIR-B, SIRPα, or SHP-2 Abs.

sine-phosphorylated complex of proteins of 130 kDa (Figure 6A, upper left panel). By contrast, in *Lyn*$^{-/-}$ cells, both the tyrosine phosphorylation of SHP-1 and the phosphorylation/association of the pp130 kDa complex were significantly reduced (Figure 6A). Immunoprecipitates of SHP-2 exhibited a similar pattern of coprecipitated proteins and again showed a significant Lyn kinase dependence in the tyrosine phosphorylation and/or association of SHP-2 with the pp130 kDa complex (Figure 6B). However, unlike SHP-1, tyrosine phosphorylation of SHP-2 was not detected in these cells. Similar results to those discussed above were also obtained in analyses of PBDMϕs (data not shown).

Others have reported that SHP-1 coimmunoprecipitates with a complex of 130 kDa phosphoproteins in Mϕ cell lines and BMMϕs. Two 130 kDa proteins complexed with SHP-1 have been identified as SIRPα (SHPS-1) and PIR-B (p91; Kubagawa et al., 1997; Timms et al., 1998; Veillette et al., 1998; Berg et al., 1998; Blery et al., 1998). Interestingly, both of these molecules are ITIM-containing Ig receptor superfamily members with demonstrated signal-inhibitory capacity (Kharitonenkov et al., 1997; Maeda et al., 1998). The model in which tyrosine phosphorylation of the cytoplasmic domains of these proteins creates binding sites for the tandem SH2 domains of SHP-1 and SHP-2 was supported by the finding that GST-SHP-2/SH2s, but not GST alone, precipitated the pp130 kDa complex from *Lyn*$^{up/up}$ BMMϕs (Figure 6C). Again, the ability of the tandem SH2 domains of SHP-2 to precipitate the pp130 kDa complex was enhanced in lysates from *Lyn*$^{up/up}$ cells and reduced in lysates from *Lyn*$^{-/-}$ cells (Figure 6C). Although we cannot rule out the presence of other p130 kDa phosphoproteins in SHP-1 and SHP-2 precipitates, both SIRPα and PIR-B exhibited enhanced tyrosine phosphorylation in *Lyn*$^{up/up}$-derived cells and conversely, were hypophosphorylated in *Lyn*$^{-/-}$ BMMϕs (Figure 6D). Moreover, the association of SHP-1/2 with PIR-B and SIRPα was enhanced in *Lyn*$^{up/up}$-derived BMMϕs (Figure 6D and data not shown).

Both SIRPα and PIR-B were also tyrosine phosphorylated when coexpressed with Lyn in 293T cells, arguing that both of these ITIM-bearing receptors may be direct substrates of Lyn (Figure 6E). We and others have shown that CSF-1 activation of c-fms leads to tyrosine phosphorylation of SIRPα (Figure 6F; Kharitonenkov et al., 1997; Timms et al., 1998). However, the Lyn-dependent SIRPα phosphorylation observed in BMMϕs was unchanged in both CSF-1-stimulated and -starved cells (data not shown). Lyn-dependent tyrosine phosphorylation of SIRPα and PIR-B in 293T cells resulted in their association with either SHP-1 or SHP-2 (Figures 6F and 6G). However, this was not the case for SHIP-1, as although Lyn expression led to the tyrosine phosphorylation of SHIP-1, SIRPα, and PIR-B, we were unable to detect either SIRPα or PIR-B in SHIP-1 precipitates from BMMϕ or 293T cell lysates (data not shown). The Lyn-dependent enhancement of tyrosine phosphorylation of both SHP-1 and SHIP-1 in *Lyn*$^{+/up}$ and *Lyn*$^{up/up}$-derived BMMϕs, and the reduction in such phosphorylation in Lyn-deficient cells, suggests that Lyn is critically involved in the membrane recruitment, intrinsic level of tyrosine phosphorylation, and the phosphorylation-associated enzymatic activity of these proteins.

Differential Recruitment of SHP-1 and SHP-2 to the Plasma Membrane in *Lyn*$^{-/-}$ and *Lyn*$^{up/up}$ BMMϕs

The ability of SHP-1 and SHP-2 to translocate from the cytoplasm to the plasma membrane is critical in terms of both recruitment of the enzymes to specific substrates and regulation of their intrinsic enzymatic activities. To investigate the differential recruitment of these molecules, we prepared crude membrane and cytosolic fractions from *Lyn*$^{+/+}$, *Lyn*$^{-/-}$, and *Lyn*$^{up/up}$ BMMϕs and assessed the compartmentalization of each protein. While Lyn, SIRPα, and PIR-B were predominantly localized to the membrane fraction in accordance with their intrinsic myristoylation and transmembrane domains, respectively, both SHP-1 and SHP-2 were unequally partitioned in the membrane and cytosol in a manner dependent on the genotype of the cells (Figure 7A). Both SHP-1 and SHP-2 were modestly enriched in the membrane fraction of *Lyn*$^{up/up}$ cells, and the level of these proteins in the membrane fraction was correspondingly diminished by approximately 50% in *Lyn*$^{-/-}$ cells (Figure 7A). In agreement with the enhanced membrane localization of SHP-1 and SHP-2, the enzymatic activity of these proteins was modestly enhanced in *Lyn*$^{up/up}$ BMMϕs (in the case of SHP-1) and correspondingly diminished by approximately 50% in *Lyn*$^{-/-}$ BMMϕs (for both SHP-1 and SHP-2) relative to *Lyn*$^{+/+}$ controls (Figure 7B). Thus, the Lyn kinase represents a critical intermediate acting to mobilize the PTPs SHP-1 and SHP-2 to the plasma membrane where they are positioned to act in establishing signaling thresholds in the myelomonocytic/Mϕ lineage (Figure 7C).

Discussion

In this study, we set out to investigate the role of the Lyn kinase in the hematopoietic system using both Lyn gain- and loss-of-function mouse models. To our surprise, mice engineered to express a constitutively activated form of Lyn containing a mutation that is oncogenic in other Src family kinases did not exhibit leukemia or tumor development. By contrast, we have shown that aged *Lyn*$^{-/-}$ mice develop severe splenomegaly and disseminated Mϕ tumors. Moreover, transfer of tumor-bearing spleen cells from *Lyn*$^{-/-}$ mice leads to the emergence of tumors within both primary and secondary SCID mice. The transplanted cells, like those of the original mouse donors, are often widely disseminated throughout the SCID mice and show a collection of features consistent with their Mϕ classification. The finding that mice lacking Lyn are prone to myeloid expansion and tumor development is intriguing. Indeed, in that Src family kinases have long been considered as protooncogenes, it would seem counterintuitive that Lyn-deficient mice develop tumors, whereas *Lyn*$^{up/up}$ mutant mice are viable and superficially healthy with no propensity toward tumor development.

In younger *Lyn*$^{-/-}$ mice, a myeloproliferative syndrome is apparent with significant increases in myeloid progenitors in spleen and peripheral blood. This phenotype is a consistent feature of all *Lyn*$^{-/-}$ mice analyzed. In agreement with the enhanced myelopoiesis in *Lyn*$^{-/-}$ mice, flow cytometric analyses showed that large num-

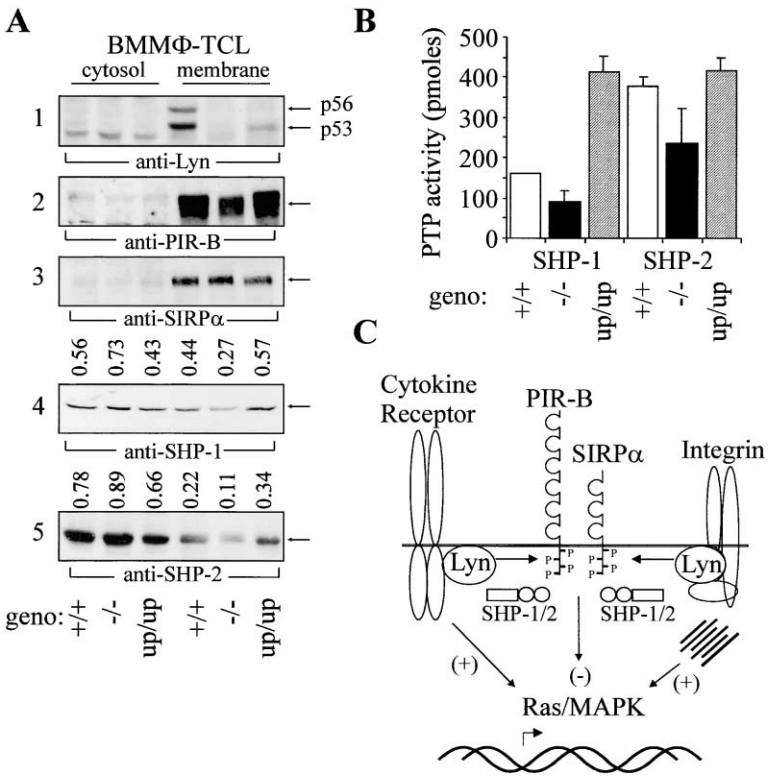

Figure 7. Lyn-Dependent Activation and Membrane Localization of SHP-1 and SHP-2

(A) BMMϕ cytosolic and membrane fractions were blotted with anti-Lyn (panel 1), anti-PIR-B (panel 2), anti-SIRPα (panel 3), anti-SHP-1 (panel 4), or anti-SHP-2 (panel 5) Abs. Relative quantities of SHP-1 and SHP-2 in each fraction were determined by densitometry and are shown above each panel.

(B) SHP-1 and SHP-2 were precipitated from BMMϕ lysates and subjected to immune complex PTP assays in the presence of Src Y416 phosphopeptide. Each point represents the mean and SD from two separate experiments.

(C) Model for Lyn-dependent mobilization of SHP-1 and SHP-2 to the plasma membrane in BMMϕs.

bers of Mϕs and neutrophils were found in the spleens of younger *Lyn*$^{-/-}$ mice. Tumor development in *Lyn*$^{-/-}$ mice has a relatively long latency (usually $\geq$30 weeks), suggesting that the myeloid expansion may become malignant due to additional acquired mutations within an expanded population of myeloid progenitors.

The splenomegaly and EMH characteristic of the *Lyn*$^{-/-}$ phenotype is similar to, although less severe than, that present in *Me*^{v}/*Me*^{v} and *SHIP-1*$^{-/-}$ mice. To date, we have not seen any reports of either SHIP-1 or SHP-1 loss-of-function mutant mice exhibiting myeloid tumor susceptibility. Although *SHIP-1*$^{-/-}$ mice do develop accumulations of myeloid cells in kidney, lung, and liver, the transplantability of this population has not been reported. Additionally, whereas the myeloid populations in *SHIP-1*$^{-/-}$ mice show characteristics typical of monocytes/Mϕs and granulocytes, tumors in *Lyn*$^{-/-}$ mice are composed of Mϕs. Both *Me*^{v}/*Me*^{v} and *SHIP-1*$^{-/-}$ mice exhibit consolidation of the lungs with myeloid cell infiltrates leading to the death of $\sim$50% of *SHIP-1*$^{-/-}$ mice by 12 weeks of age (Helgason et al., 1998; Liu et al., 1999) and the death of all *Me*^{v}/*Me*^{v} mice by 6–8 weeks (Shultz et al., 1984). By contrast, *Lyn*$^{-/-}$ mice rarely exhibit severe myeloid cell lung infiltrates. The severity of this lung pathology in *Me*^{v}/*Me*^{v} and *SHIP-1*$^{-/-}$ mice may well preclude observing age-dependent macrophage tumor development in these strains. However, heterozygous *Me*/+ mice have been reported to exhibit an increased incidence of lymphoma (Shultz et al., 1993; Bignon and Siminovitch, 1994).

In this study, we analyzed both peripheral blood and BMMϕs from both Lyn loss- and gain-of-function mutant mice to investigate the Lyn substrates and signaling pathways that may be aberrantly regulated and thus be potential predisposing elements in a pathway leading to tumor development in *Lyn*$^{-/-}$ mice. We have provided evidence that SHP-1 and SHIP-1 are differentially tyrosine phosphorylated, and that SIRPα and PIR-B are differentially associated with SHP-1 and SHP-2 in a manner dependent on the activity of Lyn in the various mouse mutants. SIRPα has been previously identified as a target of receptor tyrosine kinases and Src family kinases in vitro, and is also tyrosine phosphorylated in response to cell adhesion signals (Fujioka et al., 1996; Kharitonenkov et al., 1997; Tsuda et al., 1998; Timms et al., 1999). Importantly, expression of SIRPα has been demonstrated in BM progenitors, raising the possibility that Lyn-dependent mobilization of SH2-containing phosphatases such as SHP-1 and SHP-2 to SIRPα may be important in signal inhibition within these cells (Seiffert et al., 1999). Moreover, reduced levels of SIRPα expression are observed in a large fraction of human myeloid leukemias (Seiffert et al., 1999), and SIRPα expression potently antagonizes v-fms transformation of fibroblasts (Kharitonenkov et al., 1997). However, the possibility that defective SIRPα-dependent signal inhibition in the presence of CD47, the ubiquitously expressed ligand of SIRPα, is responsible for deregulated myelopoiesis in *Lyn*$^{-/-}$ mice remains to be evaluated (Jiang et al., 1999).

Less is known about the role of PIR-B in signal transduction, except that it is a substrate of Lyn in DT40 B cell lines and is constitutively tyrosine-phosphorylated and associated with Lyn in primary splenocytes (Maeda et al., 1998; Blery et al., 1998; Ho et al., 1999). Although it is unclear what the physiological ligand for PIR-B may be, the wide distribution of Ig superfamily ITIM-bearing

receptors such as PIR-B and SIRPα suggest a role in tempering signal transduction signals in response to a vast array of stimuli (reviewed in Ravetch and Lanier, 2000). The evidence suggesting that lack of appropriate tyrosine phosphorylation of SIRPα or PIR-B is specifically linked to the phenotype we have described is presently only correlative. Indeed, it is likely that other ITIM-bearing receptors and Lyn substrates involved in signal inhibition may also be deregulated in *Lyn*$^{-/-}$ mice. Thus, the relative contributions of diminished recruitment and/or activation of SHP-1, SHP-2, and SHIP-1 to tumor development in *Lyn*$^{-/-}$ mice will require further investigation. In this regard, previous studies have illustrated a critical role for Lyn in B lymphocytes. *Lyn*$^{-/-}$ B cells lack the full extent of the inhibitory consequences of Lyn-dependent tyrosine phosphorylation of ITIM motifs in CD22, FcγRIIB, and PIR-B, which results in a failure to recruit SHP-1, SHP-2, or SHIP-1 into the BCR complex. However, again, the relationship between the lack of phosphorylation of these individual ITIM-containing receptors and other Lyn substrate ITIM-bearing receptors such as CD5, CD72, CD66a, ILT2, -3, -4, -5, LIR8, and PD-1, and the predisposition to autoimmunity in *Lyn*$^{-/-}$ mice remains to be firmly established (reviewed in Ravetch and Lanier, 2000).

These studies of Lyn mutant mice demonstrate that a significant proportion of SHP-1, SHIP-1, PIR-B, and SIRPα tyrosine phosphorylation is regulated by Lyn in primary Mϕs. Indeed, the use of the *Lyn*^{up} mouse to explore potential Lyn substrates has illustrated its utility as a model system in this regard. Our demonstration that PTP activity may effectively compensate for the increased activity of the *Lyn*^{up} kinase mutant also illustrates potential modes of regulation, which may be lost in the process of oncogenesis. Recent work has demonstrated a role for CD45 in inhibition of tumorigenesis in low copy number p56lck^{Y505F} transgenic mice (Baker et al., 2000). We are investigating which PTP(s) might be involved in antagonizing Lyn activity. Others have shown that in BMMϕs lacking CD45, both Lyn and Hck exhibit enhanced kinase activity (Roach et al., 1997; Katagiri et al., 1995, 1999). Our preliminary data suggest that SHP-1 may be involved in the inhibition of Lyn activity (data not shown), an interaction supported by recent studies of Motheaten B cells and cell lines (Yang et al., 1998; Somani et al., 2000). This suggests that Lyn is both an activator of SHP-1 and a substrate of SHP-1-dependent negative regulation. Assessment of compound *Lyn*$^{up/up}$ *Me*^{v}/*Me*^{v} (or +/*Me*^{v}) mice will clarify this hypothesis. In light of the enhanced activation of signal-inhibitory molecules such as SHP-1 and SHIP-1 in *Lyn*$^{up/up}$ mice, it will also be interesting to explore whether *Lyn*^{up} mice are less susceptible to tumor formation induced by oncogenes such as Bcr-Abl. The possibility that Lyn kinase loss-of-function mutations may contribute to human myeloid malignancies also warrants further investigation.

Experimental Procedures

Mice and Construction of the *Lyn*^{up} (Y508F) Mutant

A targeting vector was constructed using a 5.5 kb genomic fragment derived from the 3′ end of λ*Lyn*14.1, which contains the 3′-most coding exon of the mouse *Lyn* gene and the C-terminal regulatory Tyr (Y508) (Hibbs et al., 1995b). Site-directed mutagenesis was used to introduce the *Lyn*^{Y508F} mutation and a unique XbaI restriction site immediately 3′ of the stop codon to subclone the XbaI-NheI promoter-less IRES neomycin cassette (from P. Mountford). Two homologous recombinant W9.5 ES cell lines were used to generate chimeras capable of transmitting the modified locus through the germline. Mice carrying the *Lyn*^{Y508F} point mutation were identified by PCR, confirmed by Southern blot, and bred to generate homozygous mice. Two independent strains of mice carrying the activating Y508F mutation in the *lyn* gene have been generated and analyzed. *Lyn*$^{-/-}$ mice have been described (Hibbs et al., 1995a). μ*MT*/μ*MT* mice (Kitamura and Rajewsky, 1992) were provided by D.M. Tarlinton (Walter and Eliza Hall Institute, Melbourne, Australia) and were crossed with *Lyn*$^{-/-}$ mice to create double deficient mice. Mice were housed in microisolation units.

Cells, Cell Culture, and BMMϕ Cell Growth and Survival Assays

BMMϕs were derived from cells extruded from the femurs of 8- to 12-week-old mice. Cells were flushed into DMEM supplemented with 15% heat-inactivated FCS (CSL), 20% L cell-conditioned media (LCM), 0.075% sodium bicarbonate, 50 IU/ml penicillin G, 50 μg/ml streptomycin sulfate, 2 mM Glutamax-1 (Gibco-BRL, Life Technologies), and propagated in the above media at 37°C with 10% CO_2. Nonadherent cells were removed 24 to 48 hr later and transferred into new flasks. Cells were supplemented with LCM every third day. BMMϕs were used on days 5 to 7. For BMMϕ proliferation/survival assays, day 5 to 7 cells were scraped from their dishes and plated in flat bottom 96-well plates at 5–10,000 cells/well in triplicate. Cells were grown in various concentrations of CSF-1 or GM-CSF for 3 to 5 days, and viable cells were stained with MTT as described (Harder et al., 1998). In experiments where pervanadate was used to inhibit in vivo PTP activity, sodium orthovanadate was dissolved in dH_20 to 100 mM. H_2O_2 (2 mM) was added to this 1000× stock solution, and the solution was left at room temperature for 30 min before filter sterilization and storage at −20°C. 293T cells were transiently transfected with Superfect reagent (Qiagen) according to the manufacturer's instructions. Plasmids encoding SIRPα (T. Matozaki, Kobe University, Japan), mPIR-B (T. Takai, Tohoku University, Japan), mLyn wild-type or mLyn^{Y508F}, c-fms (D. Marks, Royal Melbourne Hospital, Australia), and SHP-1 (M. Thomas, Washington University, St. Louis) were used.

Cell Lysis, Immunoblotting, and Immunoprecipitation

Cells were lysed on ice in buffer containing 1% Triton X-100, 0.1% SDS, 1% glycerol, 50 mM Tris (pH 7.5), 150 mM NaCl, 2 mM EDTA, 1 mM sodium orthovanadate, 50 mM sodium fluoride, 1 mM pefabloc, and 1 mM aprotinin. Protein concentrations were estimated using the BCA assay (Pierce). Abs used included anti-PY (4G10; UBI), anti-SIRPα (UBI), anti-PIR-B (from L. Rohrschneider, Fred Hutchinson Cancer Research Center and T. Takai, Tohoku University, Japan), anti-Lyn and anti-SHP-2 (Santa Cruz Biotechnologies), anti-Hck (from C. Lowell, University of California at San Francisco), and anti-SHP-1 (from H.-C. Cheng, University of Melbourne, Australia). In experiments requiring membrane/cytosol fractionation (Ramsby and Makowski, 1999), equal numbers of adherent BMMϕs were extracted with digitonin buffer (0.01% digitonin, 10 mM HEPES [pH 6.8], 300 mM sucrose, 100 mM NaCl, 5 mM EDTA, 3 mM $MgCl_2$, 1 mM sodium orthovanadate, and protease inhibitors) for 10 to 20 min. The adherent monolayer was then quickly rinsed in ice-cold PBS containing 1 mM vanadate before further extraction for 30 min with Triton X-100 buffer (0.5% Triton X-100, 10 mM HEPES [pH 7.4], 300 mM sucrose, 100 mM NaCl, 3 mM $MgCl_2$, 3 mM EDTA, 1 mM sodium orthovanadate, and protease inhibitors). Blots were developed with horseradish peroxidase-linked goat anti-rabbit or sheep anti-mouse antiserum and the ECL system (Amersham).

Flow Cytometry, Immunohistochemistry, and Histology

Cell preparation and FACS analysis have been described (Hibbs et al., 1995a). Lymphoid organs and tumor masses were embedded in OCT compound and frozen on dry ice. Cryostat sections (5 μM) were fixed in acetone for 10 min and air dried, and then rehydrated in PBS for 30 min. Endogenous peroxidase activity was blocked by incubation with 0.3% H_2O_2 (in PBS) for 10 min. Slides were washed in PBS, blocked in 5% FCS/PBS for 30 min before staining with the

mAbs F4/80, Mac1 (M1/70), Gr-1 (Rb6-8C5), B220 (RA3-6B2), Thy-1 (30-H12), or isotype control rat IgG2b,κ (A95-1) diluted in 5% FCS/PBS. Sections were then incubated with streptavidin-HRP conjugate (DAKO) before development with DAB chromogen solution and counterstaining with hematoxylin. For histology, tissues were fixed for light microscopy in Bouin's solution for 24 hr before paraffin embedding. Sections were stained with hematoxylin and eosin.

PTK and PTP Assays

PTP activity was detected with the malachite green microtiter plate assay as previously described (Harder et al., 1994, 1998). For Lyn kinase enzyme assays, immune complexes were washed extensively before resuspension in kinase buffer (50 mM Tris [pH 6.8], 50 mM NaCl, 0.1% Triton X-100, 10 mM $MgCl_2$, 5 mM $MnCl_2$, 25 μM ATP, 0.5 mM DTT, and 0.1 mM vanadate) containing 10 μCi [γ-^{32}P]ATP (3000 Ci/mmole) and 1–3 μg of recombinant GST-PTPα-domain2 (from F. Jirik, University of British Columbia).

Progenitor and Apoptosis Assays

Progenitor cell numbers were determined in 2 ml semisolid 0.3% agar cultures containing 10^5 spleen cells or 1.5–3.0 μl peripheral blood in 35 mm plates. Colony formation was stimulated by the presence of CSF-1 (10 ng/ml), IL-3 (10 ng/ml), GM-CSF (10 ng/ml), G-CSF (10 ng/ml), or stem cell factor (50 ng/ml). Apoptosis of BMMϕs was assessed by FACS. Briefly, treated BMMϕs in 24-well plates were rinsed twice in PBS and typsinized for 15 min. Cells and rinse solutions were combined, washed in PBS containing 2% FCS, and cells (100 μl) were stained by addition of 30 μl of a 50 μg/ml 7-AAD solution for 30 min. Percentages of apoptotic cells were assessed based on both 7-AAD fluorescence and reduced forward scatter criteria.

SCID Mouse Assays

Lyn$^{-/-}$ tumor-bearing mouse donors were assessed by palpation. Spleens exhibiting varying degrees of splenomegaly were removed, passed through a steel mesh, and resuspended in PBS. 10^7 cells were injected into the tail vein of 8- to 12-week-old female SCID mice. Tumors from SCID mice were microdissected and subjected to PCR analysis with oligonucleotides specific for the *Lyn*$^{-/-}$ mutation.

Acknowledgments

The authors are grateful to those individuals listed in the Experimental Procedures who provided reagents critical to this work. Additional thanks go to W. Alexander and L. Viney for help with peripheral blood analysis and to D. Metcalf, A. Harris, and M. Ernst for helpful discussions. Thanks also go to N. Nicola for generously providing cytokines used in this study and to D.L. Krebs and A.W. Burgess for critical review of the manuscript. Additional assistance was provided by T. Helman, E. Richardson, V. Feakes, M. Inglese, and N. Watson. K.W.H. is supported by a Terry Fox PDF Fellowship from the National Cancer Institute of Canada. M.L.H. is a recipient of a Senior Research Fellowship from the Australian Research Council. This work was supported in part by a grant from the National Health and Medical Research Council of Australia and the Cooperative Research Centre for Cellular Growth Factors.

Received April 9, 2001; revised August 2, 2001.

References

Abraham, K.M., Levin, S.D., Marth, J.D., Forbush, K.A., and Perlmutter, R.M. (1991). Thymic tumorigenesis induced by overexpression of p56lck. Proc. Natl. Acad. Sci. USA *88*, 3977–3981.

Baker, M., Gamble, J., Tooze, R., Higgins, D., Yang, F.T., O'Brien, P.C., Coleman, N., Pingel, S., Turner, M., and Alexander, D.R. (2000). Development of T-leukaemias in CD45 tyrosine phosphatase-deficient mutant lck mice. EMBO J. *19*, 4644–4654.

Berg, K.L., Carlberg, K., Rohrschneider, L.R., Siminovitch, K.A., and Stanley, E.R. (1998). The major SHP-1-binding, tyrosine-phosphorylated protein in macrophages is a member of the KIR/LIR family and an SHP-1 substrate. Oncogene *17*, 2535–2541.

Berg, K.L., Siminovitch, K.A., and Stanley, E.R. (1999). SHP-1 regulation of p62(DOK) tyrosine phosphorylation in macrophages. J. Biol. Chem. *274*, 35855–35865.

Bignon, J.S., and Siminovitch, K.A. (1994). Identification of PTP1C mutation as the genetic defect in motheaten and viable motheaten mice: a step toward defining the roles of protein tyrosine phosphatases in the regulation of hemopoietic cell differentiation and function. Clin. Immunol. Immunopathol. *73*, 168–179.

Blery, M., Kubagawa, H., Chen, C.C., Vely, F., Cooper, M.D., and Vivier, E. (1998). The paired Ig-like receptor PIR-B is an inhibitory receptor that recruits the protein-tyrosine phosphatase SHP-1. Proc. Natl. Acad. Sci. USA *95*, 2446–2451.

Briggs, S.D., Sharkey, M., Stevenson, M., and Smithgall, T.E. (1997). SH3-mediated Hck tyrosine kinase activation and fibroblast transformation by the Nef protein of HIV-1. J. Biol. Chem. *272*, 17899–17902.

Brown, M.T., and Cooper, J.A. (1996). Regulation, substrates and functions of src. Biochim. Biophys. Acta *1287*, 121–149.

Brugge, J.S., and Erikson, R.L. (1977). Identification of a transformation-specific antigen induced by an avian sarcoma virus. Nature *269*, 346–348.

Chan, V.W., Meng, F., Soriano, P., DeFranco, A.L., and Lowell, C.A. (1997). Characterization of the B lymphocyte populations in Lyn-deficient mice and the role of Lyn in signal initiation and down-regulation. Immunity *7*, 69–81.

Chan, V.W., Lowell, C.A., and DeFranco, A.L. (1998). Defective negative regulation of antigen receptor signaling in Lyn-deficient B lymphocytes. Curr. Biol. *8*, 545–553.

Chen, H.E., Chang, S., Trub, T., and Neel, B.G. (1996). Regulation of colony-stimulating factor 1 receptor signaling by the SH2 domain-containing tyrosine phosphatase SHPTP1. Mol. Cell. Biol. *16*, 3685–3697.

Corey, S.J., and Anderson, S.M. (1999). Src-related protein tyrosine kinases in hematopoiesis. Blood *93*, 1–14.

Cornall, R.J., Cyster, J.G., Hibbs, M.L., Dunn, A.R., Otipoby, K.L., Clark, E.A., and Goodnow, C.C. (1998). Polygenic autoimmune traits: Lyn, CD22, and SHP-1 are limiting elements of a biochemical pathway regulating BCR signaling and selection. Immunity *8*, 497–508.

Fujioka, Y., Matozaki, T., Noguchi, T., Iwamatsu, A., Yamao, T., Takahashi, N., Tsuda, M., Takada, T., and Kasuga, M. (1996). A novel membrane glycoprotein, SHPS-1, that binds the SH2-domain-containing protein tyrosine phosphatase SHP-2 in response to mitogens and cell adhesion. Mol. Cell. Biol. *16*, 6887–6899.

Guy, C.T., Muthuswamy, S.K., Cardiff, R.D., Soriano, P., and Muller, W.J. (1994). Activation of the c-Src tyrosine kinase is required for the induction of mammary tumors in transgenic mice. Genes Dev. *8*, 23–32.

Hakak, Y., and Martin, G.S. (1999). Ubiquitin-dependent degradation of active Src. Curr. Biol. *9*, 1039–1042.

Harder, K.W., Owen, P., Wong, L.K., Aebersold, R., Clark-Lewis, I., and Jirik, F.R. (1994). Characterization and kinetic analysis of the intracellular domain of human protein tyrosine phosphatase β (HPTP β) using synthetic phosphopeptides. Biochem. J. *298*, 395–401.

Harder, K.W., Moller, N.P., Peacock, J.W., and Jirik, F.R. (1998). Protein-tyrosine phosphatase α regulates Src family kinases and alters cell-substratum adhesion. J. Biol. Chem. *273*, 31890–31900.

Harris, K.F., Shoji, I., Cooper, E.M., Kumar, S., Oda, H., and Howley, P.M. (1999). Ubiquitin-mediated degradation of active Src tyrosine kinase. Proc. Natl. Acad. Sci. USA *96*, 13738–13743.

Helgason, C.D., Damen, J.E., Rosten, P., Grewal, R., Sorensen, P., Chappel, S.M., Borowski, A., Jirik, F., Krystal, G., and Humphries, R.K. (1998). Targeted disruption of SHIP leads to hemopoietic perturbations, lung pathology, and a shortened life span. Genes Dev. *12*, 1610–1620.

Hibbs, M.L., Stanley, E., Maglitto, R., and Dunn, A.R. (1995a). Identification of a duplication of the mouse Lyn gene. Gene *156*, 175–181.

Hibbs, M.L., Tarlinton, D.M., Armes, J., Grail, D., Hodgson, G., Maglitto, R., Stacker, S.A., and Dunn, A.R. (1995b). Multiple defects in the immune system of Lyn-deficient mice, culminating in autoimmune disease. Cell *83*, 301–311.

Ho, L.H., Uehara, T., Chen, C.C., Kubagawa, H., and Cooper, M.D. (1999). Constitutive tyrosine phosphorylation of the inhibitory paired Ig-like receptor PIR-B. Proc. Natl. Acad. Sci USA *96*, 15086–15090.

Jiang, P., Lagenaur, C.F., and Narayanan, V. (1999). Integrin-associated protein is a ligand for the P84 neural adhesion molecule. J. Biol. Chem. *274*, 559–562.

Jiao, H., Yang, W., Berrada, K., Tabrizi, M., Shultz, L., and Yi, T. (1997). Macrophages from motheaten and viable motheaten mutant mice show increased proliferative responses to GM-CSF: detection of potential HCP substrates in GM-CSF signal transduction. Exp. Hematol. *25*, 592–600.

Katagiri, T., Ogimoto, M., Hasegawa, K., Mizuno, K., and Yakura, H. (1995). Selective regulation of Lyn tyrosine kinase by CD45 in immature B cells. J. Biol. Chem. *270*, 27987–27990.

Katagiri, T., Ogimoto, M., Hasegawa, K., Arimura, Y., Mitomo, K., Okada, M., Clark, M.R., Mizuno, K., and Yakura, H. (1999). CD45 negatively regulates lyn activity by dephosphorylating both positive and negative regulatory tyrosine residues in immature B cells. J. Immunol. *163*, 1321–1326.

Kharitonenkov, A., Chen, Z., Sures, I., Wang, H., Schilling, J., and Ullrich, A. (1997). A family of proteins that inhibit signalling through tyrosine kinase receptors. Nature *386*, 181–186.

Kitamura, D., and Rajewsky, K. (1992). Targeted disruption of μ chain membrane exon causes loss of heavy-chain allelic exclusion. Nature *356*, 154–156.

Kubagawa, H., Burrows, P.D., and Cooper, M.D. (1997). A novel pair of immunoglobulin-like receptors expressed by B cells and myeloid cells. Proc. Natl. Acad. Sci USA *94*, 5261–5266.

Liu, Q., Sasaki, T., Kozieradzki, I., Wakeham, A., Itie, A., Dumont, D.J., and Penninger, J.M. (1999). SHIP is a negative regulator of growth factor receptor-mediated PKB/Akt activation and myeloid cell survival. Genes Dev. *13*, 786–791.

Maeda, A., Kurosaki, M., Ono, M., Takai, T., and Kurosaki, T. (1998). Requirement of SH2-containing protein tyrosine phosphatases SHP-1 and SHP-2 for paired immunoglobulin-like receptor B (PIR-B)-mediated inhibitory signal. J. Exp. Med. *187*, 1355–1360.

Malek, S.N., Dordai, D.I., Reim, J., Dintzis, H., and Desiderio, S. (1998). Malignant transformation of early lymphoid progenitors in mice expressing an activated Blk tyrosine kinase. Proc. Natl. Acad. Sci. USA *95*, 7351–7356.

Moarefi, I., LaFevre-Bernt, M., Sicheri, F., Huse, M., Lee, C.H., Kuriyan, J., and Miller, W.T. (1997). Activation of the Src-family tyrosine kinase Hck by SH3 domain displacement. Nature *385*, 650–653.

Nishizumi, H., Taniuchi, I., Yamanashi, Y., Kitamura, D., Ilic, D., Mori, S., Watanabe, T., and Yamamoto, T. (1995). Impaired proliferation of peripheral B cells and indication of autoimmune disease in lyn-deficient mice. Immunity *3*, 549–560.

Nishizumi, H., Horikawa, K., Mlinaric-Rascan, I., and Yamamoto, T. (1998). A double-edged kinase Lyn: a positive and negative regulator for antigen receptor-mediated signals. J. Exp. Med. *187*, 1343–1348.

Oda, H., Kumar, S., and Howley, P.M. (1999). Regulation of the Src family tyrosine kinase Blk through E6AP-mediated ubiquitination. Proc. Natl. Acad. Sci. USA *96*, 9557–9562.

Phee, H., Jacob, A., and Coggeshall, K.M. (2000). Enzymatic activity of the Src homology 2 domain-containing inositol phosphatase is regulated by a plasma membrane location. J. Biol. Chem. *275*, 19090–19097.

Ramsby, M.L., and Makowski, G.S. (1999). Differential detergent fractionation of eukaryotic cells. Analysis by two-dimensional gel electrophoresis. Methods Mol. Biol. *112*, 53–66.

Ravetch, J.V., and Lanier, L.L. (2000). Immune inhibitory receptors. Science *290*, 84–89.

Roach, T., Slater, S., Koval, M., White, L., McFarland, E.C., Okumura, M., Thomas, M., and Brown, E. (1997). CD45 regulates Src family member kinase activity associated with macrophage integrin-mediated adhesion. Curr. Biol. *7*, 408–417.

Satterthwaite, A.B., Lowell, C.A., Khan, W.N., Sideras, P., Alt, F.W., and Witte, O.N. (1998). Independent and opposing roles for Btk and lyn in B and myeloid signaling pathways. J. Exp. Med. *188*, 833–844.

Seiffert, M., Cant, C., Chen, Z., Rappold, I., Brugger, W., Kanz, L., Brown, E.J., Ullrich, A., and Buhring, H.J. (1999). Human signal-regulatory protein is expressed on normal, but not on subsets of leukemic myeloid cells and mediates cellular adhesion involving its counterreceptor CD47. Blood *94*, 3633–3643.

Shultz, L.D., Coman, D.R., Bailey, C.L., Beamer, W.G., and Sidman, C.L. (1984). "Viable motheaten," a new allele at the motheaten locus. I. Pathology. Am. J. Pathol. *116*, 179–192.

Shultz, L.D., Schweitzer, P.A., Rajan, T.V., Yi, T., Ihle, J.N., Matthews, R.J., Thomas, M.L., and Beier, D.R. (1993). Mutations at the murine motheaten locus are within the hematopoietic cell protein-tyrosine phosphatase (Hcph) gene. Cell *73*, 1445–1454.

Smith, K.G.C., Tarlinton, D.M., Doody, G.M., Hibbs, M.L., and Fearon, D.T. (1998). Inhibition of the B cell by CD22: a requirement for Lyn. J. Exp. Med. *187*, 807–811.

Somani, A.K., Yuen, K., Xu, F., Zhang, J., Branch, D.R., and Siminovitch, K.A. (2000). SH2 domain containing tyrosine phosphatase-1 downregulates activation of Lyn and Lyn-induced tyrosine phosphorylation of the CD19 receptor in B cells. J. Biol. Chem. *276*, 1938–1944.

Stehelin, D., Varmus, H.E., Bishop, J.M., and Vogt, P.K. (1976). DNA related to the transforming gene(s) of avian sarcoma viruses is present in normal avian DNA. Nature *260*, 170–173.

Takeshita, H., Taniuchi, I., Kato, J., and Watanabe, T. (1998). Abrogation of autoimmune disease in Lyn-deficient mice by the mutation of the Btk gene. Int. Immunol. *10*, 435–444.

Timms, J.F., Carlberg, K., Gu, H., Chen, H., Kamatkar, S., Nadler, M.J., Rohrschneider, L.R., and Neel, B.G. (1998). Identification of major binding proteins and substrates for the SH2-containing protein tyrosine phosphatase SHP-1 in macrophages. Mol. Cell. Biol. *18*, 3838–3850.

Timms, J.F., Swanson, K.D., Marie-Cardine, A., Raab, M., Rudd, C.E., Schraven, B., and Neel, B.G. (1999). SHPS-1 is a scaffold for assembling distinct adhesion-regulated multi-protein complexes in macrophages. Curr. Biol. *9*, 927–930.

Tsuda, M., Matozaki, T., Fukunaga, K., Fujioka, Y., Imamoto, A., Noguchi, T., Takada, T., Yamao, T., Takeda, H., Ochi, F., et al. (1998). Integrin-mediated tyrosine phosphorylation of SHPS-1 and its association with SHP-2. Roles of Fak and Src family kinases. J. Biol. Chem. *273*, 13223–13229.

Van Zant, G., and Shultz, L. (1989). Hematologic abnormalities of the immunodeficient mouse mutant, viable motheaten (mev). Exp. Hematol. *17*, 81–87.

Veillette, A., Thibaudeau, E., and Latour, S. (1998). High expression of inhibitory receptor SHPS-1 and its association with protein-tyrosine phosphatase SHP-1 in macrophages. J. Biol. Chem. *273*, 22719–22728.

Webster, M.A., Cardiff, R.D., and Muller, W.J. (1995). Induction of mammary epithelial hyperplasias and mammary tumors in transgenic mice expressing a murine mammary tumor virus/activated c-src fusion gene. Proc. Natl. Acad. Sci. USA *92*, 7849–7853.

Weissenberger, J., Steinbach, J.P., Malin, G., Spada, S., Rulicke, T., and Aguzzi, A. (1997). Development and malignant progression of astrocytomas in GFAP-v-src transgenic mice. Oncogene *14*, 2005–2013.

Yang, W., Mckenna, S.D., Jiao, H., Tabrizi, M., Lynes, M.A., Shultz, L.D., and Yi, T. (1998). SHP-1 deficiency in B-lineage cells is associated with heightened lyn protein expression and increased lyn kinase activity. Exp. Hematol. *26*, 1126–1132.

Yoshida, K., Kharbanda, S., and Kufe, D. (1999). Functional interaction between SHPTP1 and the Lyn tyrosine kinase in the apoptotic response to DNA damage. J. Biol. Chem. *274*, 34663–34668.